Session 0P4
Coherent Effects in Random Media

Validity of Kinetic Models for Waves in Random Media

G. Bal
Columbia University, USA

We consider the derivation of kinetic equations to model the correlation of two wavefields such as e.g., acoustic or electromagnetic wavefields propagating in possibly different highly heterogeneous media. The main mathematical tool in the derivation is the Wigner transform. The validity of the kinetic models is then assessed by comparing the spatial distribution of the energy density they predict with simulations of wave equations in highly heterogeneous media. The simulations are performed in two space dimensions on domains of size comparable to 500 wavelengths. This is joint work with Olivier Pinaud.

On the Intermittency of the Light Propagation in Disordered Optical Materials

Y. A. Godin and S. Molchanov
University of North Carolina at Charlotte, USA

Abstract—We consider propagation of light through an ensemble of $N \gg 1$ statistically independent optical fibers of length L whose refraction coefficient is a random function of length. We introduce the generalized transmission coefficient $|t(k,L)|^p$ for energy k^2 and study its quenched and annealed Lyapunov exponents. For small disorder we calculate the Lyapunov exponents in asymptotic form.

1. Introduction

The idea of intermittency was originally proposed in the study of turbulent flow [1] and has become widespread in statistical particle physics. Intermittency means random deviations from smooth and regular behavior. To illustrate it, we consider a bundle of N, $N \gg 1$, statistically equidistributed independent optical fibers of a fixed length L whose refractive index changes randomly along the length of the fiber. If one face of the bundle is illuminated then, due to reflection of the light and its localization in the fibers, one might expect that the outlet of the bundle will be uniformly dark. However, because of strong statistical fluctuations of the transparency (that is a typical manifestation of the intermittency), the exit of the bundle will look like a dark sky with sparse bright stars. This model was proposed by I. M. Lifshits [2] to explain high irregularity of the light distribution after propagation through a thick layer of a disordered optical material. Propagation of light in each fiber is described by the equation

$$-\psi'' + \sigma V_j(x)\psi = k^2\psi, \quad j = 1, 2, \dots, N, \tag{1}$$

where $V_j(x)$ are homogeneous random potentials equal zero outside the fibers and constant σ characterizes strength of the disorder.

Equation 1 has scattering solutions

$$\psi_{k,j}(x) = \begin{cases} e^{ikx} + r_j(k)\, e^{-ikx}, & x < 0, \\ t_j(k)\, e^{ikx}, & x > L, \end{cases} \tag{2}$$

where $t_j(k)$ and $r_j(k)$ are random complex transmission and reflection coefficients, respectively, such that $|t_j(k)|^2 + |r_j(k)|^2 = 1$. We also introduce the empirical mean $\frac{1}{N}\sum_{j=1}^{N} |t_j(k)|^2$ for the transmitted energy provided the energy density of the incident wave equals one for each waveguide, and for fixed L and $N \to \infty$

$$\frac{1}{N}\sum_{j=1}^{N} |t_j(k)|^2 \xrightarrow{a.s.} \langle |t(k,L)|^2 \rangle, \tag{3}$$

where a.s. means almost surely (with probability one). Expressions $|t(k,L)|^p$ and $\langle |t(k,L)|^p \rangle$ are decreasing exponentially as $L \to \infty$ whose logarithmic rate of decay we call the quenched and annealed (moment) transmission Lyapunov exponents, respectively,

$$\gamma_q^T(k,p) = \lim_{L\to\infty} \frac{\ln |t(k,L)|^p}{L} = p \lim_{L\to\infty} \frac{\ln |t(k,L)|}{L} = p\gamma^T(k), \tag{4}$$

$$\mu_a^T(k,p) = \lim_{L\to\infty} \frac{\ln\langle |t(k,L)|^p \rangle}{L}. \tag{5}$$

Using this notation we can quantitatively characterize intermittency: after propagation through the fiber bundle light exhibits intermittency if

$$|\mu_a^T(k,2)| < |\gamma_q^T(k,2)|. \tag{6}$$

The stronger inequality (6) is, the more intermittent is the distribution of energy on the exit of the fiber bundle.

2. Analytical Tools

The study of equation 1 with representative potential $V(x)$ is based on the phase-amplitude formalism. Let $\psi_k^{(i)}(x), i = 1, 2$, be the fundamental set of solutions of (1) with initial values $\psi_k^{(1)}(0) = 1$, $\frac{d}{dx}\psi_k^{(1)}(0) = 0$, $\psi_k^{(2)}(0) = 0$, $\frac{d}{dx}\psi_k^{(2)}(0) = 1$. The matrix

$$M_k([0, L]) = \begin{pmatrix} \psi_k^{(1)}(L) & k\psi_k^{(2)}(L) \\ \frac{1}{k}\frac{d}{dx}\psi_k^{(1)}(L) & \frac{d}{dx}\psi_k^{(2)}(L) \end{pmatrix} \tag{7}$$

is the propagator of (1) whose determinant equals one.

For the general solution of (1) we put

$$\psi_k(x) = r_k(x)\sin\theta_k(x), \quad \frac{d\psi_k(x)}{dx} = kr_k(x)\cos\theta_k(x). \tag{8}$$

Then for θ_k and $\ln r_k$ we obtain the following system [2], [3]

$$\frac{d\theta_k(x)}{dx} = k - \frac{\sigma V(x)\sin^2\theta_k}{k}, \tag{9}$$

$$\frac{d\ln r_k(x)}{dx} = \frac{1}{2k}\sin 2\theta_k(x)V(x). \tag{10}$$

In most cases of interest [2], [3], the phase $\theta_k(x) \in [0, \pi)$ represents either a Markov process with generator $\mathcal{L}$ (white noise potential) or a component of a multidimensional Markov process (the Kronig-Penny model). To illustrate intermittent behavior of light distribution, we use the simplest case when the potential $V(x) = \dot{b}(x)$ is the white noise (the derivative of the Brownian motion $b(x)$).

Equations 9–10 are understood as Itô's stochastic differential equations with Stratonovich corrections. In our case, the generator of the diffusion process (9) has the form [4]

$$(\mathcal{L}f)(\theta) = \frac{B^2(\theta)}{2}\frac{d^2f}{d\theta^2} + \left(A(\theta) + \frac{(BB')(\theta)}{2}\right)\frac{df}{d\theta}, \tag{11}$$

where $A(\theta) = k$, $B(\theta) = -\dfrac{\sigma\sin^2\theta}{k}$. Similarly,

$$d(\ln r(x)) = \left(\alpha(\theta(x)) + \frac{1}{2}\beta B(\theta(x))\right)dx + \beta\left(\theta(x)\right)\cdot db(x) \tag{12}$$

with $\alpha = 0$ and $\beta(\theta) = \dfrac{\sigma\sin 2\theta}{2k}$. Hence,

$$r^p(x) = e^{\int_0^x D(\theta)\cdot db(z) + \int_0^x C(\theta)\,dz}, \tag{13}$$

where $D(\theta) = p\beta(\theta(z))$ and $C(\theta) = p(\alpha + \frac{1}{2}\beta B)(\theta(z))\,dz$. If $u_p(x, \theta) = \langle r^p(x)|\theta(0) = \theta\rangle$ is the expectation of $r^p(x)$, then $u_p(x, \theta)$ satisfies the Feynman-Kac formula which for the white noise potential has the form

$$\frac{\partial u_p}{\partial x} = \frac{\sigma^2\sin^4\theta}{2k^2}\frac{\partial^2 u_p}{\partial\theta^2} + \left(k + \frac{\sigma^2(1-p)\sin^2\theta\sin 2\theta}{2k^2}\right)\frac{\partial u_p}{\partial\theta} + \frac{\sigma^2 p\sin^2\theta\cos\theta(p\cos\theta - \sin\theta)}{2k^2}u_p = \widetilde{\mathcal{L}}_p u_p. \tag{14}$$

Formula (14) allows to calculate the Lyapunov exponent for the amplitude $r(L)$. In the quenched case we have

$$\begin{aligned}\frac{\ln r(L)}{L} &= \frac{1}{L}\int_0^L \frac{1}{2}\beta B(\theta(x))\,dx + \beta(\theta(x))\cdot db(x) \xrightarrow{a.s.} \langle\frac{1}{2}\beta B\rangle_\eta \\ &= -\frac{\sigma^2}{4k^2}\int_0^\pi \eta(\theta)\sin 2\theta\sin^2\theta\,d\theta = \gamma_q(k).\end{aligned} \tag{15}$$

Here $\eta(\theta)d\theta$ is the invariant measure for the phase $\theta(x)$ which satisfies the equation

$$\mathcal{L}^*\eta = \frac{d^2}{d\theta^2}\left(\frac{\sigma^2\sin^4\theta}{2k^2}\eta\right) - \frac{d}{d\theta}\left[\left(k + \frac{\sigma^2\sin^2\theta\sin 2\theta}{2k^2}\right)\eta\right] = 0 \tag{16}$$

that can be solved exactly.

Consider now the moment Lyapunov exponent

$$\mu_a(p) = \lim_{L\to\infty} \frac{\ln\langle r^p(L)\rangle}{L}. \tag{17}$$

According to Perron–Frobenius theorem about positive semigroups, $\mu_a(p)$ equals maximum eigenvalue of the nonsymmetric operator $\widetilde{\mathcal{L}}_p$ (14)

$$\widetilde{\mathcal{L}}_p \psi = \mu_a(p)\psi \tag{18}$$

and the corresponding eigenfunction $\psi(x)$ is strictly positive.

The Lyapunov exponent $\gamma(k)$ of the amplitude $r(L)$ and $\mu(p)$ have the following properties:

(a) $\gamma(k) > 0$. This property leads to the localization theorem for the Hamiltonian $H\psi = -\psi'' + \sigma V(x)\psi = \lambda\psi$ on the whole real axis [2], [3].

(b) For fixed k the annealed Lyapunov exponent is analytic in p and convex.

(c) $\mu(p)$ is symmetric with respect to $p = -1$: $\mu(p) = \mu(-p-2)$ and $\frac{d\mu}{dp}(0) = \gamma(k)$. In particular, $\mu(0) = \mu(-2) = 0$ (Fig. 1).

(d) For small disorder constant σ and fixed k $\gamma(k) = \frac{\pi\sigma^2 \widehat{B}(2k)}{4k^2}(1 + o(\sigma))$, where $\widehat{B}(2k)$ is the spectral density of the potential V. For the white noise $\gamma(k) = \frac{\sigma^2}{8k^2}(1 + o(\sigma))$ and $\mu_a(p) \approx \frac{1}{2}p(p+2)\sigma^2\gamma(k)$ as $\sigma \to 0$.

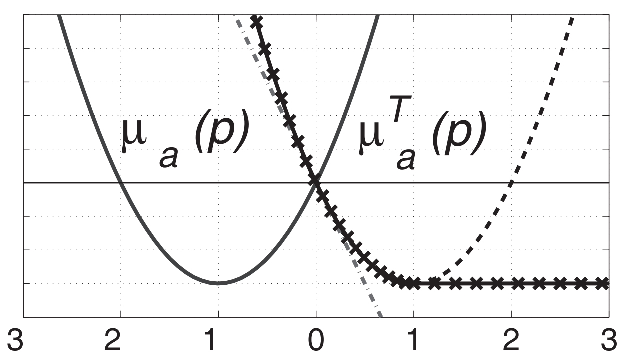

Figure 1: Graphs of the annealed moment Lyapunov exponent $\mu_a(p)$ (solid line) and transmission Lyapunov exponent $\mu_a^T(p)$ (crossed line) for fixed k and small σ.

The energy transmission coefficient can be calculated through the matrix $M_k([0, L])$ (7) as follows

$$|t(k, L)|^2 = \frac{4}{2 + \|M_k([0, L])\|^2}, \tag{19}$$

where the norm is understood as the sum of the squares of matrix's entries. Then $\|M_k([0, L])\|^2 = [r_k^{(1)}(L)]^2 + [r_k^{(2)}(L)]^2$. From asymptotic behavior of the amplitudes $\ln r_k^{(i)}(L) \approx \gamma(k)L, \quad i = 1, 2$, with probability one as $L \to \infty$ we conclude that $\ln \|M_k([0, L])\| \approx \gamma(k)L$. Therefore,

$$\frac{\ln|t(k, L)|}{L} = \frac{1}{L} \ln \sqrt{\frac{4}{2 + \|M_k([0, L])\|^2}} \to -\gamma(k). \tag{20}$$

Thus, the quenched transmission Lyapunov exponent is

$$\mu_q^T(k, p) = \lim_{L\to\infty} \frac{\ln|t(k, L)|^p}{L} = -p\gamma(k) < 0. \tag{21}$$

Calculation of the annealed Lyapunov exponent is more difficult. Typically $r_k \sim e^{L\gamma(k)}$. However, with exponentially small probability $r_k(L)$ can be of the order $e^{-\delta L}, \quad \delta > 0$. Then $\langle r_k^p(L)\rangle = e^{-p\delta L} P\{\ln r_k(L) < -\delta L\}$, and for very negative p the product tends to $+\infty$ (Fig. 1). We use large deviation theory [5] to calculate $\mu_a^T(k, p)$. Let us take $0 \leq \beta < \gamma$ and estimate $P\{r_k(L) < e^{\beta L}\}$. Using exponential Chebyshev inequality with optimization over parameter $p \leq 0$ we obtain

$$P\{r_k(L) < e^{\beta L}\} = P\{r_k^p(L) > e^{p\beta L}\} \leq \min_{p\leq 0} \frac{\langle r_k^p(L)\rangle}{e^{p\beta L}} \sim \min_{p\leq 0} e^{(\mu_a(k,p)-p\beta)L} = e^{\mu^*(k,p)L}, \tag{22}$$

where $\mu^*(k,\beta) = \max_p(-p\beta + \mu_a(k,p))$ is the Legendre transform [6] of $\mu(k,p)$ for fixed k with respect to parameter p. It is well-known that in the Markov case it is not only estimation from above but the logarithmic equivalence: $P\{r_k < e^{\beta L}\} \overset{\log}{\sim} e^{-\mu^*(k,p)L}$. Now for $p > 0$

$$\langle |t(k,L)|^p\rangle \overset{\log}{\sim} \int \frac{1}{e^{-p\beta L} + e^{p\beta L}}\, dP\{r_k < e^{\beta L}\} = \max_{0\leq\beta\leq\gamma} e^{-p\beta L - \mu^*(k,\beta)} = \begin{cases} e^{\mu(k,-p)L}, & 0 < p \leq 1, \\ e^{\mu(k,-1)L}, & p > 1. \end{cases} \tag{23}$$

For small σ we can use parabolic approximation for $\mu_a^T(k,p)$ that gives

$$\gamma_q^T(k,p) = -p\frac{\pi\widehat{B}(2k)}{4k^2}\sigma^2(1+o(1)) \tag{24}$$

and

$$\mu_a^T(k,p) = \begin{cases} p(p+2)\dfrac{\pi\widehat{B}(2k)}{8k^2}\sigma^2(1+o(1)), & p \leq 1, \\ -\dfrac{\pi\widehat{B}(2k)}{4k^2}\sigma^2(1+o(1)), & p > 1, \end{cases} \tag{25}$$

where $B(x) = \mathrm{Cov}(V(y)V(y+x))$ is the covariance of random potential $V(x)$, and $\widehat{B}(k) = \dfrac{1}{2\pi}\displaystyle\int_{-\infty}^{\infty} e^{-ikx}B(x)\,dx$ is the corresponding energy spectrum of $V(x)$ (Fig. 1). In particular, for $p = 2$

$$\mu_a^T(k,2) \approx \frac{1}{4}\,\gamma_q^T(k,2) < 0. \tag{26}$$

This relation is the manifestation of the strong intermittency (cf. [1]). It shows that the main contribution to the transmitted energy comes not from "typical" fibers where the logarithmic rate of energy decay is $\gamma_q^T(k,2)$, but rather from few rare fibers (the probability of their occurrence is $e^{\frac{1}{4}\gamma_q^T(k,2)L}$) through which significant part of the energy of order $O(1)$ is transmitted. Thus, we have the I. M. Lifshits picture described in the introduction.

3. Conclusion

We have considered propagation of light through a bundle of independent optical fibers whose refractive index is a random function of length. It is found that distribution of energy at the exit of the bundle has intermittent behavior. For quantitative estimation of irregularity we introduced the generalized energy transmission coefficient and studied its Lyapunov exponent. Essential difference in the quenched and annealed energy transmission Lyapunov exponents is suggested as a manifestation of intermittency. In the case of small randomness of the fiber refractive index it is found that the energy transmission Lyapunov exponent of a typical single fiber is four times bigger than the average one of the bundle. Unlike the moment Lyapunov exponent $\mu_a(p)$ for the amplitude which has quadratic dependence on the moment p, the transmission moment Lyapunov exponent is constant for $p \geq 1$.

REFERENCES

1. Zeldovich, Y. B., S. A. Molchanov, A. A. Ruzmaikin, and D. D. Sokoloff, "Intermittency, diffusion and generation in a non-stationary random media," *Sov. Sci. Rev., Sec. C*, Vol. 7, 1–110, 1988.
2. Lifshits, I. M., S. A. Gredescul, and L. A. Pastur, *Introduction to the Theory of Disordered Systems*, John Wiley, New York, 1988.
3. Pastur, L. A. and A. Figotin, *Spectra of Random and Almost Periodic Operators*, Springer-Verlag, New York, 1992.
4. Ikeda, N. and S. Watanabe, *Stochastic Differential Equations and Diffusion Processes*, Elsevier, 1989.
5. Freidlin, M. A. and A. D. Wentzell, *Random Perturbations of Dynamical Systems*, Springer-Verlag, New York, 1998.
6. Arnold, V. I., *Mathematical Methods of Classical Mechanics*, Springer-Verlag, New York, 1978.

Model of the Electromagnetic Contribution to Wurface Enhanced Raman Scattering (SERS)

V. Giannini, **J. A. Sánchez-Gil**, **and J. V. García-Ramos**
Consejo Superior de Investigaciones Científicas, Spain

E. R. Méndez
División de Física Aplicada, México

In this work, we present a theoretical model of the electromagnetic contribution to surface enhanced Raman scattering (SERS). The SERS effect is characterized by the enormous intensification of the Raman emission of molecules, when these are adsorbed on a metallic surface (with nanometric roughness). This intensification is several orders of magnitude higher than the Raman emission of isolated molecules. In recent years, SERS spectroscopy has improved in sensitivity so as to make possible the detection of a single molecule on a nanostructured substrate [1]. The SERS effect is due to the combined action of chemical and electromagnetic enhancement mechanisms. Leaving aside the contribution of the chemical mechanism, this is possible provided that there is a huge concentration of electromagnetic field on certain points of the substrate, due to the excitation and localization of surface plasmons [2–4].

We thus investigate the electromagnetic mechanism that is responsible for such surface-plasmonind-uced, electromagnetic field enhancements. Our theoretical model incorporates the Raman response of a metallic surface covered with a dipole layer. The calculation of the scattered electromagnetic field is based on the exact Green's theorem integral equation formulation. With this model we are able to calculate the surface field, near field, and far field at the Raman-shifted frequency, separately of the electromagnetic field at pump frequency. A rigorous calculation of the scattered electromagnetic field has been carried out for random metal surfaces with similar properties to those exhibited by nanostructured metal substrates used in SERS. Numerical results are presented for single realizations, along with mean values of the SERS enhancement factor averaged over an ensemble of realizations [1].

REFERENCES

1. Nie, S. and S. R. Emory, "Probing single molecules and single nanoparticles by surface-enhanced raman scattering," *Science*, Vol. 275, 1102, 1997, and K. Kneipp, Y. Wang, H. Kneipp, L. T. Perlman, I. Itzkan, R. R. Dasari, and M. S. Feld, "Single molecule detection using surface-enhanced Raman scattering (SERS)," *Phys. Rev. Lett.*, Vol. 78, 1667, 1997.
2. Barnes, W., A. Dereux, and T. Ebbesen, "Surface plasmon subwavelength optics," *Nature*, Vol. 424, 824 2003.
3. Sánchez-Gil, J. A., J. V. García-Ramos, and E. M éndez, "Near-field electromagnetic wave scattering from random self-affine fractal metal surfaces: Spectral dependence of local field enhancements and their statistics in connection with surface-enhanced raman scattering," *Phys. Rev. B*, Vol. 62, 10515, 2000.
4. Sánchez-Gil, J. A., "Localized surface-plasmon polaritons in disordered nanostructured metal surfaces: Shape versus Anderson-localized resonances," *Phys. Rev. B*, Vol. 68, 113410, 2003.
5. Giannini, V., J. A. Sánchez-Gil, J. V. García-Ramos, and E. Médez, "Theoretical model of the electromagnetic contribution to surface enhanced Raman scattering (SERS)," *preprint.*

The Local Density of States in Finite Size Photonic Structures, Small Particles Approach

V. Prosentsov
University of Twente, The Netherlands

A. Lagendijk
FOM-Institute for Atomic and Molecular Physics, The Netherlands

We study the local density of states in finite size photonic structures by considering them as made of small particles. Dividing the structure into segments with a size small compared to the incident wavelength, one can apply methods suitable for the wave scattering by small particles. This local perturbation method correctly reproduces the lowest frequency resonance of the small particles and it fulfills the optical theorem (energy conservation). The small particles can be given prescribed positions in space: for instance random, or periodic as in a photonic crystal. By using the local perturbation method, we have calculated the local density of states for one, two, and three dimensional finite size photonic structures.

Spatial Wave Intensity and Field Correlations in Quasi-one-dimensional Wires

G. Cwilich
Yeshiva University, USA

Spatial intensity correlations between waves transmitted through random media are analyzed within the framework of the random matrix theory of transport. Assuming that the statistical distribution of transfer matrices is isotropic, we found that the spatial correlation function of the normalized intensity can be expressed as the sum of three terms, with distinctive spatial dependences. This result coincides with the one obtained in the diffusive regime from perturbative calculations, (Patrick Sebbah et al. in Phys. Rev. Lett. 88, 123901, 2002), but holds all the way from quasi-ballistic transport to localization. It is only the specific value of the coefficients which depends on the specific transport regime. Their values obtained from the Monte Carlo solution of the Dorokhov, Mello, Pereyra, and Kumar (DMPK) scaling equation are in full agreement with microscopic numerical calculations of bulk disordered wires. The experimental and numerical results are recovered inh the large-N (number of propagating channels) limit in Random Matrix theory. While correlations are positive in the diffusive regime, we predict a transition to negative correlations as the length of the system decreases.

Near-field Intensity Correlations in Semicontinuous Metal-dielectric Films

H. Cao[1], **K. Seal**[1], **A. K. Sarychev**[2], **D. A. Genov**[3]
V. M. Shalaev[3], **A. Yamilov**[1], **H. Noh**[1], **and Z. C. Ying**[4]

[1]Northwestern University, USA
[2]Ethertronics Inc., USA
[3]Purdue University, USA
[4]National Institute of Standards and Technology, USA

Spatial correlations of field and intensity are indicative of the nature of wave transport in random media and have been widely investigated in the context of electromagnetic wave propagation in disordered dielectric systems However, less is known of near-field intensity correlations in metallic random systems, which can exhibit rich phenomena due the involvement of intrinsic resonance effects-surface plasmons. Neither is clear the difference between correlation functions in metallic and dielectric systems.

This paper presents the first experimental study of near-field intensity correlations in metal-dielectric systems in regimes where localization and delocalization are expected. Significant differences are observed between the spatial intensity correlations functions in metal-dielectric systems and those of purely dielectric random media.

In disordered metallic nanostructures, surface plasmon modes are governed by the structural properties of the system and may be strongly localized. Recent theoretical studies of metallic nanoparticle aggregates suggest that the eigenmodes of such systems may have properties of both localized and delocalized states. However, it is not clear how such eigenmodes impact the propagation or localization of surface plasmon polaritons excited by impinging light, an issue addressed in this study. In the current experiment, the concentration of metal particles on a dielectric surface p was varied over a wide range to control the amount of scattering. Spatial intensity correlations obtained from near-field optical microscopy (NSOM) images show a transition from propagation to localization and back to propagation of optical excitations in planar random metal-dielectric systems with increase in metal filling fraction.

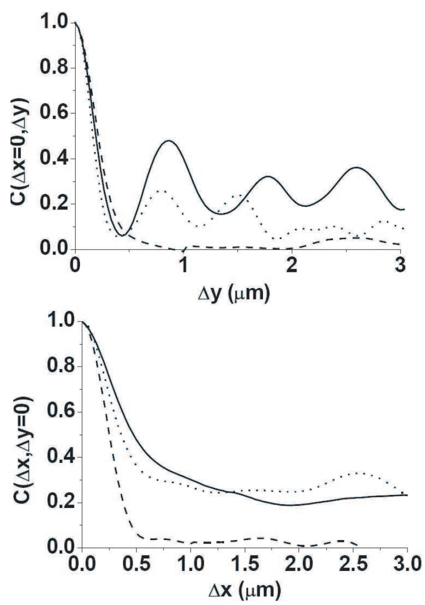

Figure 1: $C(0, \Delta y)$ and $C(\Delta x, 0)$ at $p = 0.36$ solid line), 0.65 (dashed line) and 0.83 (dotted line). For comparison, all curves are normalized to a value of unity.

Semicontinuous silver films on glass substrates were synthesized by pulsed laser deposition. Samples were illuminated by the evanescent field (in the total internal reflection geometry) of He-Ne lasers, and the local optical signal was collected by a fiber tip. From the near-field images, we computed the 2D correlation functions for near-field intensities. Fig. 1 shows the intensity correlation functions in the directions parallel and perpendicular to the incident wave vector $k_{\|}$, i.e., $C(0, \Delta y)$ and $C(\Delta x, 0)$. Along $k_{\|}$, $C(0, \Delta y)$ exhibits oscillatory behavior at $p = 0.36$ with a period of 870 nm. This oscillation is replaced by a monotonic decay at $p = 0.65$. At $p = 0.83$, the oscillations reappear with a smaller period of 690 nm. The presence of oscillations in $C(0, \Delta y)$ is an indication of wave propagation along the y-axis. This propagation is suppressed at $p = 0.65$, suggesting localization of near-field energy. Therefore, the existence, suppression and reappearance of the oscillations in the near-field intensity correlation function with increasing p correspond to a gradual transition from propagation to localization and back to propagation of optical excitations in the samples. Note that the oscillation periods observed above are always larger than λ, in contrast with purely dielectric media, which exhibit damped oscillations with a period of $\lambda/2$.

Cones, Spirals, and Möbius Strips in Multiply Scattered Light

I. Freund
Bar-Ilan University, Israel

Laser light scattered by a multiple scatterer invariably emerges elliptically polarized. In general, the orientations of the ellipses in elliptically polarized light vary throughout space. In three dimensions the orientation of an ellipse may be described by a 3-frame in which one frame axis is along the major axis of the ellipse, a second frame axis is along the minor axis of the ellipse, and the third frame axis is along the normal to the ellipse. These three axes are shown to generate cones, spirals, and Möius strips, characterized by a total of 27 different topological indices.

For ordinary ellipses (the vast majority) that are not on singular lines of circular or linear polarization, the Möbius strips have one full twist, and there are a total of 21 indices that are non zero. These indices, if independent, could collectively divide the field into $2^{21} = 2,097,152$ structurally different grains separated by grain boundaries on which an index becomes undefined. Selection rules, however, reduce the number of independent configurations to 140,608, while within a linear approximation for the local field surrounding an ellipse there exist degeneracies that further reduce the number of distinguishable configurations to 17,360. Of these, 1,728 are of first order, and should be readily accessible to experiments using recently developed optical near field methods.

Analytical expressions have been obtained for all indices in terms of the 20 parameters needed to define a general field of ellipses within the linear approximation, and more than 10,000 different configurations have been harvested in a simulated multiply scattered random field (speckle pattern), demonstrating that large numbers of configurations can be expected appear in practice.

This previously unsuspected, indeed unprecedented, structural proliferation is intrinsic to spatially varying elliptically polarized light, and in addition to random fields, is found in the fields of wave guides that support a small number of modes (2–3), as well as in the highly ordered fields of optical lattices. Other systems described locally by spatially varying 3-frames, such as liquid crystals, or the dielectric constants of continuous random media, can be expected to show a similar degree of structural proliferation.

Absorption Induced Confinement of Lasing Modes in Diffusive Random Medium

A. Yamilov[1], **A. L. Burin**[2], **X. H. Wu**[1], and **H. Cao**[1]

[1]Northwestern Unversity, USA
[2]Tulane University, USA

Tight focusing of pump light on a weakly scatting (diffusive) random medium can lead to lasing with coherent feedback [1]. Imaging of laser light on the sample surface revealed that the lasing modes were not extended over the entire random medium, instead they were located inside the pumped region with an exponential tail outside of it [2]. Since the quasimodes of a random system far from the onset of localization are usually extended states, the origin of the localized lasing modes is not clear.

We use FDTD method to simulate lasing in TM modes of 2D random media. The disordered system is a collection of dielectric cylinders placed at random in vacuum. The lateral dimension of 2D random system is $9.2\,\mu$m. Transport mean free path $l \simeq 1.3\,\mu\text{m} \ll L$, so that the system is in the diffusive regime. By assigning negative conductance (inside cylinders) to the pumped region and positive conductance to unpumped region, we are able to include both light amplification and reabsorption of the emitted light.

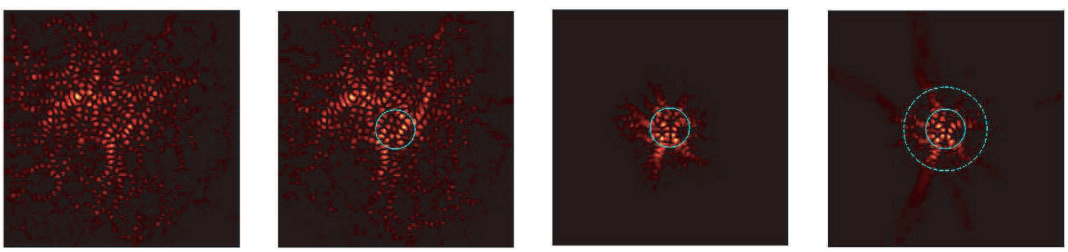

(a) (b) (c) (d)

Figure 1: Mode modification in the presence of reabsorption (see text).

Fig. 1(a) shows spatial intensity distribution of the (extended) quasimode with the longest lifetime in a passive diffusive system. in Fig. 1(b) we show the (first) lasing mode with gain inside the circular region near the center and no absorption outside. Although optical gain is local, the lasing mode is extended throughout the entire sample-the lasing mode profile remains the same as in Fig. 1(a). The lasing mode in the presence of reabsorption outside the circle, Fig. 1(c), is a new mode, completely different from the quasimode of the passive system. It is confined inside the pumped region, and shows an exponential decay outside. The reabsorption suppresses the feedback from absorbing part of the sample, effectively reducing the system size to V_{eff}. Indeed, Fig. 1(d) depicts the lasing mode when we remove all the random medium beyond one diffusive absorption length from the pump area (dashed circle). The frequency and spatial profile of the lasing mode remain the same as in Fig. 1(c).

This reduction of the effective system volume leads to a decrease of the Thouless number $\delta \equiv \delta\nu/\Delta\nu$, where $\delta\nu$ and $\Delta\nu$ are the average mode linewidth and spacing respectively. In a 3D diffusive system $\delta\nu \propto V_{eff}^{-2/3}$ and $\delta\nu \propto V_{eff}^{-1}$, therefore, $\delta \propto V_{eff}^{1/3}$. The smaller the value of δ, the larger the fluctuation of the decay rates γ of the quasimodes. We believe the broadening of the decay rate distribution along with the decrease of the total number of quasimodes (within V_{eff}) is responsible for the observation of discrete lasing peaks in the regime of tight focusing of pump beam [1].

REFERENCES

1. Cao, H., *Wave Random Media*, Vol. 13, R1, 2003.
2. Cao, H., Y. Ling, J. Y. Xu, and A. L. Burin, *Phys. Rev. E*, Vol. 66, R05601, 2002.

Exploiting Multiple Scattering of Waves in Random Media

J. A. Scales and K. van Wijk
Colorado School of Mines, USA

In this talk we describe our experimental work in the measurment of phase-coherent multiple scattering of waves in random media. We use a wide variety of non-contacting optical, millimeter wave and ultrasonic techniques to probe natural random media (such as rocks) as well as artificial systems. By using non-contacting methods we can record dense, high-fidelity data sets which sample the random fluctuations of the media. By carefully measuring the phase of these waves as well as their amplitude, we can exploit mesoscale fluctuations to achieve resolution beyond diffusion and radiative transfer, which neglect this phase information.

Coherent-potential-approximation Multiple-scattering Scheme for the Study of Photonic Crystals with Substitutional Disorder

V. Yannopapas
University of Patras, Greece

Photonic crystals of spherical scatterers have been theoretically studied using the the layer Korringa-Kohn-Rostoker (LKKR) method [1, 2] which is ideally suited for the calculation of the transmission, reflection and absorption coefficients of an electromagnetic (EM) wave incident on a composite slab consisting of a number of planes of non-overlapping particles with the same two-dimensional (2D) periodicity. For each plane of particles, LKKR calculates the full multipole expansion of the total multiply scattered wave field and deduces the corresponding transmission and reflection matrices in the plane-wave basis. The transmission and reflection matrices of the composite slab are evaluated from those of the constituent layers. In this study we present a photonic version of the coherent-potential approximation (CPA) [3, 4] for the study of photonic crystals with substitutional disorder (photonic alloys) within the LKKR context. The CPA method has been extensively used in the study of the electronic properties of disordered atomic alloys [5, 6] and is expected to give reasonably good results at least in the case of moderate disorder. It is the best approach for studying the properties of a disordered photonic crystal by means of substituting it with an effective periodic one whose properties correspond, on the average, to those of the actual disordered photonic crystal. The CPA-LKKR method is applied to case of dielectric photonic crystals of both cermet, i.e., opals, and network topology, i.e., inverted opals, as well as to the case of metallo-dielectric photonic crystals in order to determine an effective permittivity in the long-wavelength limit. The method is also used for the calculation of the transmission/ reflection and absorption coefficients of light incident on finite slabs of disordered photonic crystals.

REFERENCES

1. Stefanou, N., V. Yannopapas, and A. Modinos, "Heterostructures of photonic crystals: frequency bands and transmission coefficients," *Comput. Phys. Commun.*, Vol. 113, No. 1, 49–77, 1998.
2. Stefanou, N., V. Yannopapas, and A. Modinos, "MULTEM 2: A new version of the program for transmission and band-structure calculations of photonic crystals," *Comput. Phys. Commun.*, Vol. 132, No. 1–2, 189–196, 2000.
3. Stefanou, N. and A. Modinos, "Scattering of electromagnetic waves by a disordered two-dimensional array of spheres," *J. Phys. Condens. Matter*, Vol. 5, No. 47, 8859–8868, 1993.
4. Modinos, A., V. Yannopapas, and N. Stefanou, "Scattering of electromagnetic waves by nearly periodic structures," *Phys. Rev. B*, Vol. 61, No. 12, 8099–8107, 2000.
5. Phariseau, P., B. L. Györffy, and L. Scheire (editors), *Electrons in Disordered Metals and at Metallic Surfaces*, Plenum, New York, 1979.
6. Gonis, A., *Green Functions for Ordered and Disordered Systems*, North-Holland, Amsterdam, 1992.

Two-dimensional Randomly Rough Surfaces that Act as Gaussian Schell-model Sources

E. R. Méndez
División de Física Aplicada, Mexico

T. A. Leskova and A. A. Maradudin
University of California, USA

We consider the scattering of a scalar Gaussian beam of frequency ω incident normally on a twodimensional randomly rough surface defined by $x_3 = \zeta(\mathrm{x}_\parallel)$, where $\mathrm{x}_\parallel = (x_1, x_2, 0)$. The region $x_3 > \zeta(\mathrm{x}_\parallel)$ is vacuum while the region $x_3 < \zeta(\mathrm{x}_\parallel)$ is the scattering medium. We assume that the Dirichlet boundary condition is satisfied on the surface $x_3 = \zeta(\mathrm{x}_\parallel)$. We denote the scattered field in the vacuum region by $\Phi(\mathrm{x}|\omega)_{sc}$, and its value on the plane $x_3 = 0$, by $\Phi(\mathrm{x}_\parallel|\omega)_{sc}$. We seek the surface profile function $\zeta(\mathrm{x}_\parallel)$ for which $\Phi(\mathrm{x}_\parallel|\omega)_{sc}$ satisfies the condition $\langle\Phi(\mathrm{x}_\parallel|\omega)_{sc})\Phi^*(\mathrm{x}_\parallel|\omega)_{sc}\rangle = A^2\exp(-\mathrm{x}_\parallel^2/4\sigma^2)\exp[-(\mathrm{x}_\parallel - \mathrm{x}_\parallel^{'})^2/2\sigma_\mathrm{g}^2]\exp(-\mathrm{x}_\parallel^{'2}/4\sigma_\mathrm{s}^2)$, where the angle brackets denote an average over the ensemble of realizations of $\zeta(\mathrm{x}_\parallel)$. Such a surface is a Gaussian Schell-model source of radiation. The field scattered from the resulting surface, although it is only partically coherent, has the intensity distribution of a fully coherent laser beam whose intensity in the plane $x_3 = 0$ has the form $A_L^2\exp(-2\mathrm{x}_\parallel^2/\delta_\mathrm{L}^2)$, where $\delta_L = 2\sigma_s\sigma_g/(\sigma_g^2 + \sigma_s^2)^{1/2}$ and $A_L\delta_L = 2A\sigma_s$.

Two approaches are used to determine the surface profile function that acts as a Gaussian Schellmodel source. Both are based on the geometrical optics limit of the phase perturbation theory expression for the scattered field. In the first approach the surface profile function $\zeta(\mathrm{x}_\parallel)$ is represented as a continuous array of triangular facets. The joint probability density function of two orthogonal slopes of each facet is determined from the condition that the field scattered from the resulting surface has the desired correlation property in the plane $x_3 = 0$. In the second approach it is shown that a surface profile function $\zeta(\mathrm{x}_\parallel)$ that is a stationary, zero-mean, isotropic, Gaussian random process, can also act as a Gaussian Schell-model source, when the rms height and transverse correlation length of the surface roughness are suitably chosen. Each of these two approaches is validated by the results of numerical simulation calculations of the intensity distribution of the scattered field, which show that it indeed has the form of a laser beam.

The Design of Two-dimensional Randomly Rough Surfaces with Specified Scattering Properties: Non-normal Incidence

A. A. Maradudin and T. A. Leskova
University of California, USA

In a recent paper [1] a method was proposed for designing a two-dimensional randomly rough surface on which the Dirichlet boundary condition is satisfied that, when illuminated at normal incidence by a scalar plane wave, produces a scattered field whose mean differential reflection coefficient has a specified dependence on the scattering angles. The method was based on the geometrical optics limit of the Kirchhoff approximation. The mean plane of the surface, the x_1x_2 plane, was tessellated by equilateral triangles. For x_1 and x_2 within a given triangle the surface profile function $\zeta(x_1x_2)$ was assumed to be a linear function of x_1 and x_2 of the form $b^{(0)} + a^{(1)}x_1 + a^{(2)}x_2$. The pair of slopes $a^{(1)}$ and $a^{(2)}$ for a given triangle were assumed to be random deviates that were independent of the pair of slopes for any other triangle, and all pairs of $a^{(1)}$ and $a^{(2)}$ had the same joint probability density function. The amplitude $b^{(0)}$ was determined by making the surface continuous. The mean differential reflection coefficient was found to be given in terms of this joint probability density function. This relation could be inverted to yield the joint probability density function in terms of the mean differential reflection coefficient that the surface was intended to produce. From the joint probability density function for $a^{(1)}$ and $a^{(2)}$ the marginal probability density functions were obtained, as well as the conditional probability for $a^{(2)}$ given $a^{(1)}$, and vice versa. The rejection method [2] was then used with these marginal and conditional probability density functions to construct an ensemble of realizations of the random surface. In the present work we extend the approach proposed in [1] to the case of non-normal incidence, and illustrate it by applying it to the design of a surface that scatters a plane wave in such a way as to produce a mean scattered intensity that is constant within a rectangular region of scattering angles, and produces no scattering outside this region. It is validated by the results of numerical simulation calculations.

REFERENCES

1. Méndez, E. R., T. A. Leskova, A. A. Maradudin, M. Leyva-Lucero, and J. Muñoz-Lopez, *J. Opt.*, A7, S141, 2005.
2. Press, W. H., S. A. Teukolsky, W. T. Vetterling, and B. P. Flannery, *Numerical Recipes in Fortran, 2nd Edition*, 281–282, Cambridge University Press, New York, 1992.